

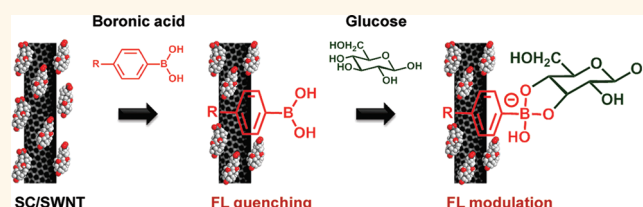
# Boronic Acid Library for Selective, Reversible Near-Infrared Fluorescence Quenching of Surfactant Suspended Single-Walled Carbon Nanotubes in Response to Glucose

Kyungsuk Yum,<sup>†,§</sup> Jin-Ho Ahn,<sup>†,§</sup> Thomas P. McNicholas,<sup>†</sup> Paul W. Barone,<sup>†</sup> Bin Mu,<sup>†</sup> Jong-Ho Kim,<sup>†,‡</sup> Rishabh M. Jain,<sup>†</sup> and Michael S. Strano<sup>†,\*</sup>

<sup>†</sup>Department of Chemical Engineering, Massachusetts Institute of Technology, Cambridge, Massachusetts 02139, United States and <sup>‡</sup>Department of Chemical Engineering, Hanyang University, Ansan 426-791, Republic of Korea. <sup>§</sup>These authors contributed equally to this work.

Single-walled carbon nanotubes (SWNTs) emit a stable fluorescence at near-infrared (nIR) wavelengths.<sup>1,2</sup> The fluorescence of SWNTs is highly responsive to their physical and chemical environment, making SWNTs a highly sensitive platform for biological and chemical sensing.<sup>3–6</sup> For example, SWNTs have been used as nIR optical sensors for glucose,<sup>4,7</sup> nitric oxide,<sup>5</sup> nitroaromatics,<sup>8</sup> and proteins<sup>9,10</sup> through the selective modulation of the SWNT fluorescence upon binding of target analytes, even at the single-molecule level.<sup>11–13</sup> Particularly, the nonphotobleaching, nIR fluorescence of SWNTs provides unique advantages in biological environments over conventional fluorophores, which typically photobleach and emit fluorescence at visible wavelengths, because biological tissues are optically transparent and minimally autofluorescent at nIR wavelengths.<sup>14</sup> Because the direct covalent attachment of receptor chemistries to the nanotube surface invariably extinguishes fluorescent emission from SWNTs, noncovalent and indirect methods of functionalization are required to render SWNTs selective to analyte binding. High-throughput analysis methods, where libraries of homologous molecules are screened and compared for efficacy, have proven valuable for drug discovery and catalytic development. The application of high-throughput analysis methods to the problem of optical sensor development can provide structural and chemical clues to the most effective ways of transducing analyte binding to optically modulate SWNTs. In this work, we develop and apply a library

## ABSTRACT



We describe the high-throughput screening of a library of 30 boronic acid derivatives to form complexes with sodium cholate suspended single-walled carbon nanotubes (SWNTs) to screen for their ability to reversibly report glucose binding *via* a change in SWNT fluorescence. The screening identifies 4-cyanophenylboronic acid which uniquely causes a reversible wavelength red shift in SWNT emission. The results also identify 4-chlorophenylboronic acid which demonstrates a turn-on fluorescence response when complexed with SWNTs upon glucose binding in the physiological range of glucose concentration. The mechanism of fluorescence modulation in both of these cases is revealed to be a photoinduced excited-state electron transfer that can be disrupted by boronate ion formation upon glucose binding. The results allow for the elucidation of design rules for such sensors, as we find that glucose recognition and transduction is enabled by para-substituted, electron-withdrawing phenyl boronic acids that are sufficiently hydrophobic to adsorb to the nanotube surface.

**KEYWORDS:** single-walled carbon nanotubes · near-infrared fluorescence · near-infrared optical sensor · boronic acids · glucose

of boronic acid (BA) constructs to sodium cholate suspended SWNTs (SC/SWNTs) and screen the resulting complexes for their ability to modulate fluorescence emission in response to glucose. An examination of successful candidates yields structural and chemical design rules to enable such sensors.

Boronic acids are an excellent molecular receptor for saccharides.<sup>15,16</sup> The detection

\* Address correspondence to strano@mit.edu.

Received for review November 7, 2011 and accepted December 2, 2011.

Published online December 02, 2011 10.1021/nn204323f

© 2011 American Chemical Society

and monitoring of saccharides (e.g., glucose and fructose) is vital in medical diagnostics, biomedical research, and biotechnology.<sup>15–17</sup> Boronic acids have attracted attention as an alternative receptor to enzymes for saccharide detection (e.g., glucose oxidases for glucose detection).<sup>17–19</sup> The enzyme-based sensing has the disadvantages that, since it is based on the rate of the reaction between the enzyme and the analyte, this approach is sensitive to various factors that affect the enzyme activity and the mass transport of the analyte, it consumes the analyte, and it requires mediators; in contrast, the boronic-acid-based sensing is based on the reversible and equilibrium-based complexation of boronic acids and saccharides, thus consuming no analytes.<sup>17,19</sup>

The reversible complexation of saccharides with aromatic boronic acids produces a stable boronate anion, changing the electronic properties of the boronic acids, such as the reduction potential of aromatic boronic acids.<sup>17,19–21</sup> This alternation in the electronic properties of aromatic boronic acids upon binding of saccharides has been a basic scheme for various boronic-acid-based saccharide sensing approaches, including electrochemical,<sup>17,19,20</sup> fluorescence,<sup>16,18,22</sup> and colorimetric measurements.<sup>23</sup> We thus hypothesized that the complexation of saccharides with aromatic boronic acids conjugated on the surface of SWNTs, presumably through  $\pi$ – $\pi$  interactions between the graphene sidewall of SWNTs and the aromatic moiety of the boronic acids, could modulate the SWNT fluorescence signal in response to binding of saccharides. Here we report the first application of high-throughput screening to the study of the reactivity of SWNTs, using a library of 30 aromatic boronic acids (listed in Table 1) and the fluorescence spectral response of these 30 boronic acid–SWNT (BA–SWNT) complexes to glucose addition (our model analyte in this study) in aqueous solutions (Figure 1). We found that the fluorescence of BA–SWNT complexes, quenched by the attachment of boronic acids to nanotubes, can be selectively recovered in response to the binding of glucose in the physiological range of glucose concentrations. The reversible fluorescence quenching of the BA–SWNT complex that exploits boronic acids as a molecular receptor provides a new strategy for SWNT-based highly stable and sensitive nIR optical sensing of saccharides, building upon our earlier work.<sup>4,5,7,8,13</sup> Particularly, the optical sensing of glucose holds promise for noninvasive *in vivo* continuous glucose monitoring, important for diabetes management; however, this ultimate goal of glucose monitoring has yet to be realized.<sup>24,25</sup> For instance, commercial noninvasive continuous glucose monitors for long-term use are not currently available.<sup>25</sup> With the non-photobleaching, nIR fluorescence of SWNTs, the SWNT-based nIR optical sensing of glucose has great potential in this regard.

## RESULTS AND DISCUSSION

To identify boronic acids that can be exploited as a molecular receptor for saccharides in SWNT-based sensing systems, we screened the fluorescence spectral response of SC/SWNT solutions against 30 boronic acids (listed in Table 1) and the subsequent spectral change of the 30 BA–SWNT complexes in response to glucose in aqueous solutions (Figure 1). Figure 2 shows representative fluorescence spectra that compare the original spectrum of SC/SWNTs (black), the spectrum after adding 50 mM boronic acids to the SC/SWNT solutions (blue), and the spectrum after adding 50 mM glucose to the BA–SWNT complex solutions (red). The addition of boronic acids resulted in a fluorescence loss and/or an emission wavelength shift of SWNT fluorescence (blue lines in Figure 2): the BA–SWNT complex of 4-chlorophenylboronic acid (BA2) and 4-cyanophenylboronic acid (BA9) shows both the fluorescence loss and the red shift of the emission wavelength, whereas the BA–SWNT complex of 9,9-dihexylfluorene-2,7-diboronic acid (BA16) and indazole-6-boronic acid (BA30) only shows the fluorescence loss. The subsequent addition of a model analyte (glucose in our study) to the BA–SWNT complex solutions also caused a fluorescence intensity change (red lines in Figure 2): the nanotube fluorescence either recovered (BA2, BA9, and BA16) or further decreased (BA30). The fluorescence recovery of the BA–SWNT complex of 4-cyanophenylboronic acid (BA9) upon introduction of glucose also accompanied a blue shift of the emission wavelength (Figure 2b). This wavelength shift, or solvatochromism,<sup>26,27</sup> is generally rare among SWNT optical responses to molecular binding.

Figure 3 summarizes the fluorescence intensity change and the wavelength shift of (6,5) nanotubes upon addition of 30 different aromatic boronic acids (50 mM) (Figure 3a) and subsequent addition of glucose (50 mM) to the 30 BA–SWNT complexes (Figure 3b). All 30 boronic acids studied here induced some nanotube fluorescence loss, suggesting the adsorption of the boronic acids to the nanotube sidewall through the surfactant layer. This adsorption is mediated through the anticipated  $\pi$ – $\pi$  interactions between the sidewall of SWNTs and the aromatic moiety of the boronic acids. We note that 14 boronic acids also caused a significant red shift of the emission wavelength upon initial adsorption. The subsequent addition of glucose to the 30 BA–SWNT complex solutions changed the nanotube fluorescence intensity and/or the emission wavelength only for some specific boronic acid structures, which we analyze in more detail below. The addition of dimethyl sulfoxide (DMSO) to SC/SWNT solutions and the addition of glucose to SC/SWNT solutions without boronic acids did not change the fluorescence spectrum of nanotubes (Supporting Information Figure S1). Moreover, the fluorescence emission of

TABLE 1. Library of Boronic Acids

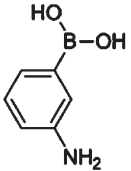
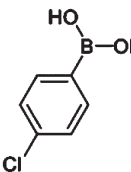
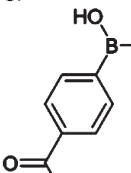
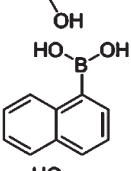
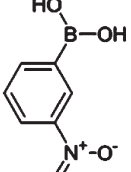
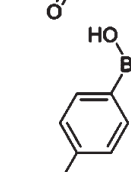
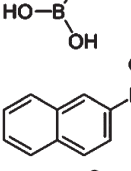
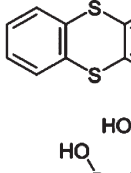
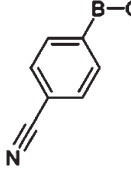
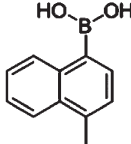
Entry	Boronic acid	Structure
BA1	3-Aminophenylboronic acid	
BA2	4-chlorophenylboronic acid	
BA3	4-carboxyphenylboronic acid	
BA4	Naphthalene-1-boronic acid	
BA5	3-Nitrophenylboronic acid	
BA6	Benzene-1,4-diboronic acid	
BA7	2-Naphthylboronic acid	
BA8	1-Thianthrenylboronic acid	
BA9	4-Cyanophenylboronic acid	
BA10	4-Methyl-1-naphthaleneboronic acid	

TABLE 1. CONTINUED

Entry	Boronic acid	Structure
BA11	6-Methoxy-2-naphthaleneboronic acid	
BA12	6-Ethoxy-2-naphthaleneboronic acid	
BA13	3-Biphenylboronic acid	
BA14	8-Quinolinylnboronic acid	
BA15	Pyrene-1-boronic acid	
BA16	9,9-Dihexylfluorene-2,7-diboronic acid	
BA17	Acenaphthene-5-boronic acid	
BA18	10-Bromoanthracene-9-boronic acid	
BA19	4-(Diphenylamino)phenylboronic acid	
BA20	4-(4'-Methoxybenzyloxy)phenylboronic acid	

TABLE 1. CONTINUED

Entry	Boronic acid	Structure
BA21	4-(4'-(2-Pentyloxy)phenyl)phenylboronic acid	
BA22	2-(tert-Butyldimethylsilyloxy)naphthalene-6-boronic acid	
BA23	9-Anthraceneboronic acid	
BA24	5-Bromopyridine-3-boronic acid	
BA25	9-Phenanthracenylboronic acid	
BA26	4-Bromo-1-naphthaleneboronic acid	
BA27	2-Aminopyrimidine-5-boronic acid	
BA28	Indazole-4-boronic acid hydrochloride	
BA29	Fluorene-2-boronic acid	
BA30	Indazole-6-boronic acid	

boronic acids is very small in the wavelength range of our interest (Supporting Figure S2).

Generally, we find that the greatest modulation of SWNT emission occurs for cases where the initial

boronic acid adsorption yields a large fluorescence quenching (>50% of the initial value.) This observation, combined with the fact that glucose invariably increases the resulting emission intensity upon binding,

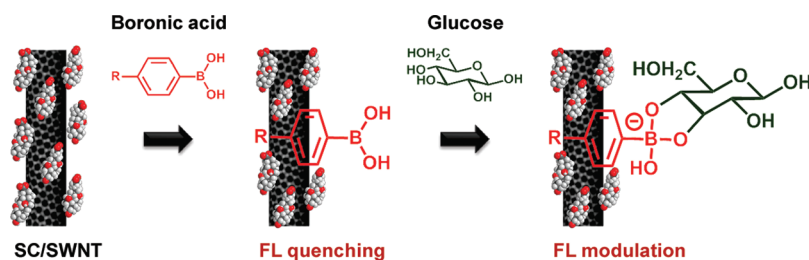


Figure 1. Schematic illustration of the reaction of boronic acids with sodium cholate suspended SWNTs (SC/SWNTs) and the fluorescence (FL) spectral response of the boronic acid–SWNT complex to glucose.

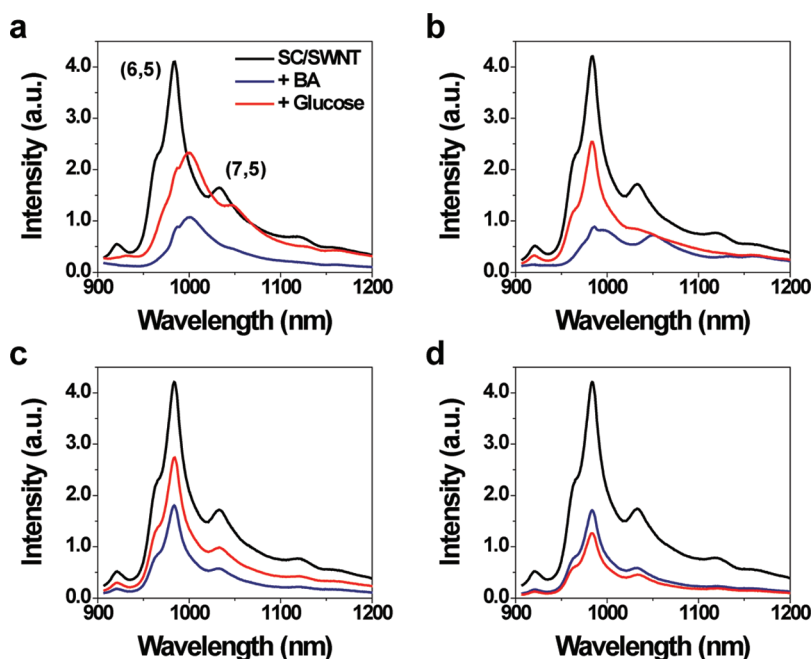


Figure 2. Representative fluorescence spectra that compare the original spectrum of SC/SWNTs (black), the spectrum after adding 50 mM boronic acids to SC/SWNT solutions (blue), and the spectrum after adding 50 mM glucose to the BA–SWNT complex solutions (red). The BA–SWNT complexes were prepared with 4-chlorophenylboronic acid (BA2) (a), 4-cyanophenylboronic acid (BA9) (b), 9,9-dihexylfluorene-2,7-diboronic acid (BA16) (c), and indazole-6-boronic acid (BA30) (d).

allows us to assign the general mechanism as follows. The boronic acid adsorbs on the nanotube sidewall, through  $\pi$ – $\pi$  stacking interactions with the pendant aromatic moiety, causing a fluorescence quenching. Glucose binding disrupts this interaction, partially restoring the decreased emission.

An interesting candidate boronic acid uncovered in this work is 4-cyanophenylboronic acid (BA9), which causes a relatively rare solvatochromic shift in response to glucose as well as a large intensity change (Figure 2b). Figure 4a shows the fluorescence spectra of the BA–SWNT complex of 4-cyanophenylboronic acid (BA9) upon stepwise addition of the boronic acid to SC/SWNT solutions (see also Supporting Figure S3). The stepwise addition of the boronic acid attenuated the nanotube fluorescence and red-shifted the emission wavelength. A significant red shift begins to clearly appear at the boronic acid concentration of 38.5 mM for (6,5) nanotubes and, interestingly, at a lower boronic acid concentration of 9.9 mM for (7,5)

nanotubes (Figure 4a). The stepwise addition of DMSO to SC/SWNT solutions did not change the fluorescence spectrum (Supporting Figures S1 and S3).

To assign the mechanism of fluorescence modulation, we next measured the absorbance spectrum of the BA–SWNT complex solutions for different concentrations of 4-cyanophenylboronic acid (BA9) (Figure 4b). Despite the significant fluorescence loss and wavelength shift observed when the boronic acid was added, the absorbance spectra show no change. We also observed a similar behavior with 4-chlorophenylboronic acid (BA2): despite a significant change in the fluorescence spectrum, the BA–SWNT complex of 4-chlorophenylboronic acid (BA2) also shows constant absorbance spectrum (Supporting Figure S4). The addition of DMSO to SC/SWNTs and the addition of glucose to SC/SWNTs without boronic acids did not change the absorbance spectrum (Supporting Figure S1). The absorbance of the boronic acids themselves is very small in the wavelength range of our interest (Supporting Figure S2).

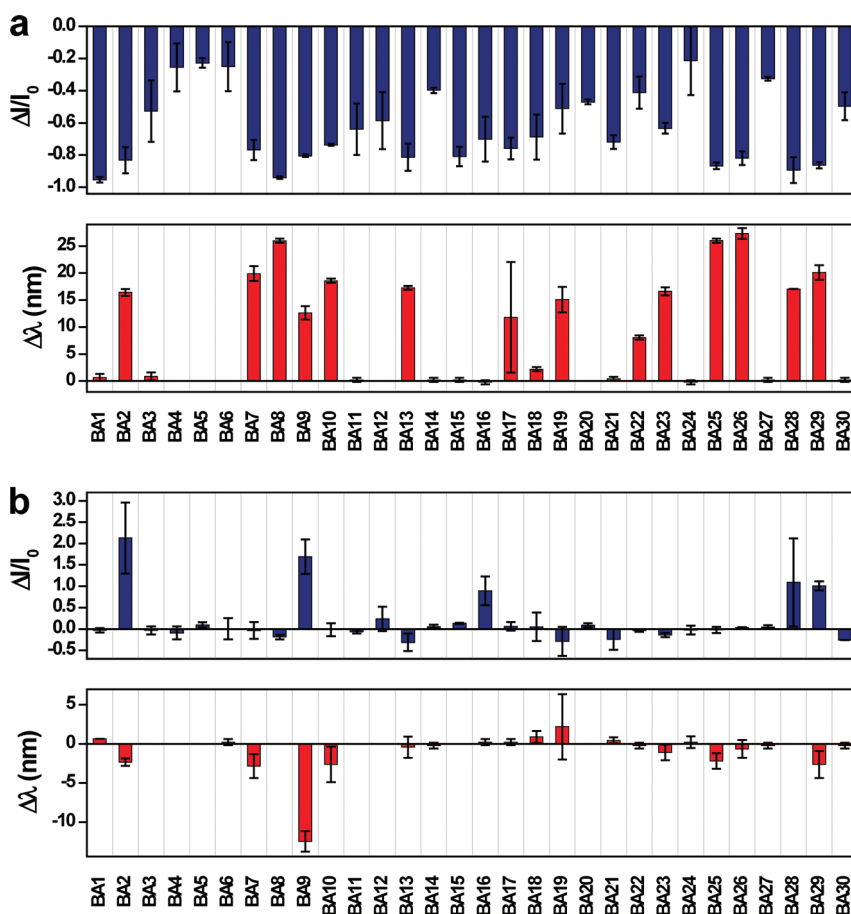
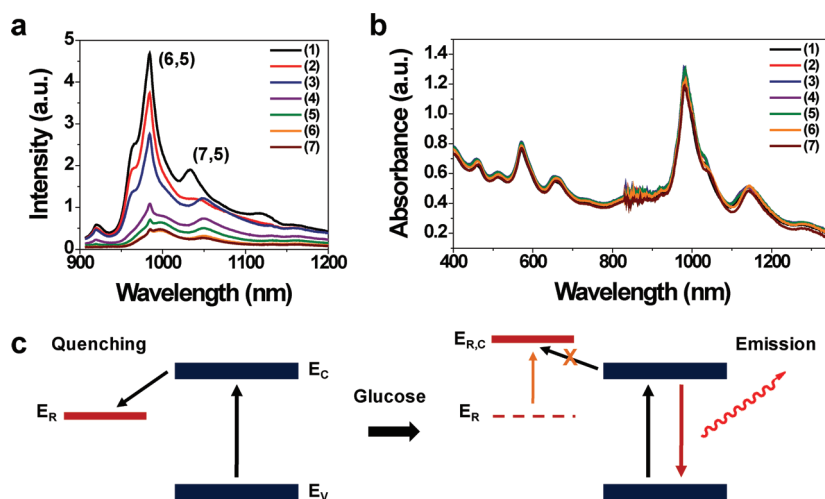


Figure 3. High-throughput screening of the reactivity of SWNTs with a library of 30 boronic acids (listed in Table 1) and the fluorescence response of the 30 BA–SWNT complex to glucose. (a) Fluorescence intensity change (top) and wavelength shift (bottom) of (6,5) nanotubes after the addition of 30 different aromatic boronic acids of 50 mM. (b) Fluorescence intensity change (top) and wavelength shift (bottom) of (6,5) nanotubes after the subsequent addition of 50 mM glucose to the 30 BA–SWNT complexes shown in (a). The error bars are the standard deviation of at least three measurements.

We therefore assign the mechanism of fluorescence intensity loss as a photoinduced excited-state electron transfer from the SWNT conduction band to the boronic acids nonradiatively (*i.e.*, quenching),<sup>9</sup> rather than from a decrease in transition strength (transition bleaching)<sup>28</sup> (as schematically described in Figure 4c). Previous studies<sup>28</sup> reported that fluorescence bleaching, through a mechanism of a ground-state electron transfer from the nanotube to the oxidizing agent, accompanies a similar loss in the absorbance spectrum. The fluorescence quenching mechanism in our study is also supported by the observation that the red shift of the emission wavelength of (7,5) nanotube begins to appear at a lower boronic acid concentration than that of the (6,5) nanotube. The fluorescence quenching through the excited-state electron transfer mechanism is energetically favorable for large diameter nanotubes with a smaller band gap because of a larger potential difference between the nanotube conduction band and the boronic reduction potential; the Fermi level of SWNTs becomes more negative with the increase of SWNT diameters (*i.e.*, with the decrease of SWNT band gaps).<sup>9,28,29</sup> Additionally, the constant absorbance indicates that the fluorescence

quenching and red shift process does not involve the aggregation of SWNTs. We may attribute the variation in the quenching of nanotubes for different boronic acids to both the different affinity between boronic acids and nanotubes and the different reduction potential of boronic acids relative to the potential of nanotubes.

The reversible fluorescence quenching of the BA–SWNT complex in response to saccharides can provide a new strategy for SWNT-based nIR optical sensing, particularly for glucose. To verify the potential use of this “turn-on” sensing scheme, in which the binding of saccharides to the boronic acid receptor of the BA–SWNT complex increases the nanotube fluorescence, we quantified the fluorescence recovery upon addition of glucose. Because the complexation is reversible and reagentless, the binding of saccharides to the aromatic boronic acids is expected to be a function of saccharide concentration. To maximize the sensitivity of the BA–SWNT complex, we first determined an optimal level of the boronic acid that maximizes the coverage on the nanotube surface (and thus maximizes the fluorescence quenching), while minimizing free boronic acids



**Figure 4.** Fluorescence quenching upon introduction of 4-cyanophenylboronic acid (BA9) and fluorescence quenching and recovery mechanisms of the BA–SWNT complex. (a) Fluorescence spectra of nanotubes, showing fluorescence quenching upon stepwise addition of the boronic acid (BA9): (1) starting nanotubes, and after adding the boronic acid of 9.9 mM (2), 19.6 mM (3), 29.1 mM (4), 38.5 mM (5), 47.6 mM (6), and 56.6 mM (7). (b) Absorbance spectra of nanotubes during the quenching process: (1) starting nanotubes, and after adding the boronic acid (BA9) of 5 mM (2), 10 mM (3), 15 mM (4), 25 mM (5), 40 mM (6), and 50 mM (7). (c) Fluorescence quenching mechanism in the absence of glucose (left): a photoinduced excited electron transfer from the nanotube to the boronic acid. Fluorescence recovery mechanism in the presence of glucose (right): upon the complexation of glucose with the boronic acid, the reduction potential of the complexed boronic acid shifts to a more negative value, which makes the excited electron transfer from the nanotube to the boronic acid less favorable or impossible, thus leading to fluorescence recovery.

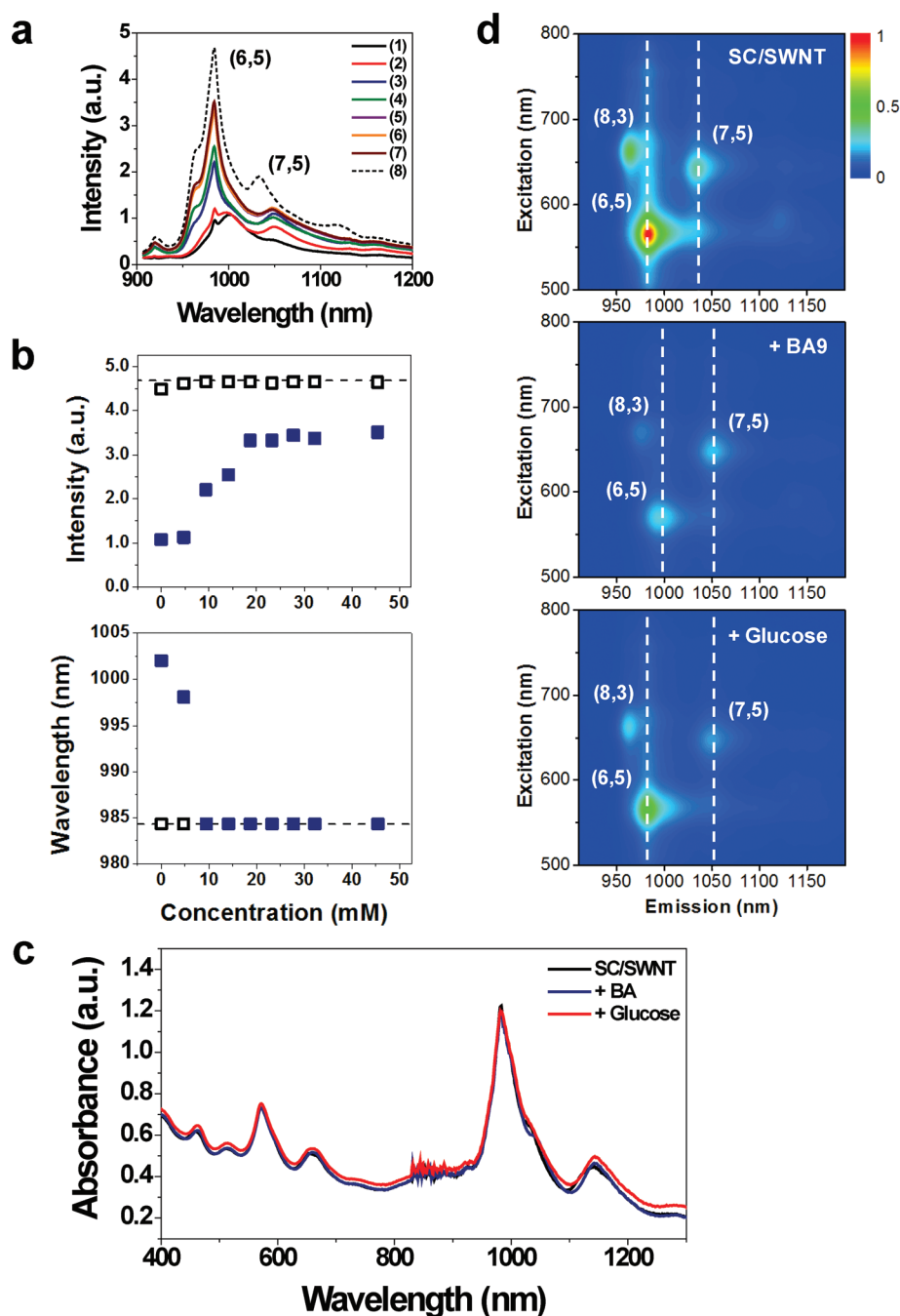
that are not conjugated with nanotubes in a solution.<sup>9</sup> The free boronic acids can also bind with the target analyte, which can interfere with the complexation of the analyte with the receptor boronic acid on the nanotube surface, limiting the sensitivity of the BA–SWNT complex. For 4-cyanophenylboronic acid (BA9), we determined an optimal concentration level of 40 to 50 mM; the fluorescence quenching was saturated at this concentration range (Figure 4a and Supporting Figure S3).

Figure 5a shows the fluorescence spectra of the quenched BA–SWNT complex of 4-cyanophenylboronic acid (BA9) upon stepwise introduction of glucose. As determined above, we prepared the BA–SWNT complex solution with the boronic acid concentration of 50 mM. The BA–SWNT complex gradually recovers the quenched fluorescence and the red-shifted emission wavelength with the increase of glucose concentration (Figure 5a). Figure 5b shows the fluorescence intensity (top) and the emission wavelength (bottom) of (6,5) nanotubes as a function of glucose concentration (blue square). The addition of 45.5 mM glucose recovered the nanotube fluorescence to a saturated level, reaching 75% of the original SC/SWNT fluorescence level (dashed black line in Figure 5b). We also observed a similar behavior for the BA–SWNT complex of 4-chlorophenylboronic acid (BA2) (Supporting Figure S4). Remarkably, the BA–SWNT complexes can sense the glucose concentration in a physiologically important range (0–30 mM), allowing a potential use of this reversible fluorescence quenching and wavelength shift of the BA–SWNT complex for nIR optical

sensors for glucose monitoring. Figure 5c compares the absorbance spectra of the BA–SWNT complex in the absence and in the presence of glucose and the absorbance spectrum of the starting SC/SWNT. The absorbance spectrum does not show any change upon the addition of glucose, implying that the fluorescence recovery in the presence of glucose does not involve the aggregation and redispersion of nanotubes. Figure 5d shows the excitation profile maps of SC/SWNTs (top), the same nanotube sample after adding 50 mM 4-cyanophenylboronic acid (BA9) (middle) and after subsequently adding 50 mM glucose (bottom), clearly showing the reversible quenching of the nanotube fluorescence and/or the reversible shift of the emission wavelength.

We attribute the mechanism of the fluorescence recovery to the change in the electronic properties of the aromatic moiety of the boronic acid upon binding of glucose (as illustrated in Figure 4c). The complexation of saccharides with aromatic boronic acids switches boronic acids from a trigonal neutral form with an  $sp^2$  boron atom (an electron-deficient Lewis acid) to a tetrahedral boronate anionic form with an electron-rich  $sp^3$  boron atom (increasing its inductive electron-donating ability) at the pH range of 6 to 9.<sup>16,17,19,21</sup> This complexation hence alters the reduction potential of the boronic acid more negatively,<sup>17,20</sup> which reduces or reverses the potential difference between the nanotube conduction band and the reduction potential of the boronic acid and can thus make an excited electron transfer from the nanotube to the boronic acid





**Figure 5.** Fluorescence recovery of the quenched BA-SWNT complex of 4-cyanophenylboronic acid (BA9) in the presence of glucose. (a) Fluorescence spectra upon stepwise addition of glucose: starting BA-SWNT complex prepared with 4-cyanophenylboronic acid (BA9) of 50 mM (1), and after the addition of glucose of 4.7 mM (2), 9.4 mM (3), 14.1 mM (4), 18.7 mM (5), 23.3 mM (6), and 45.5 mM (7). The dashed black line (8) shows the original spectrum of SC/SWNTs. (b) Peak fluorescence intensity (top) and emission wavelength (bottom) of (6,5) nanotubes of the BA-SWNT complex (shown in panel a) as a function of glucose concentration (blue). The black open square shows the fluorescence intensity (top) and wavelength (bottom) of (6,5) nanotubes of SC/SWNTs without boronic acids as a function of glucose concentration: glucose was added stepwise to the SC/SWNTs without boronic acids. The dashed black line shows the fluorescence intensity (top) and wavelength (bottom) of (6,5) nanotubes of the original SC/SWNTs. (c) Absorbance spectra of the original SC/SWNTs (black), and the BA-SWNT complex in the absence (blue) and in the presence of glucose of 54.1 mM (red). (d) Excitation profile maps of SC/SWNTs (top), the same nanotube sample after the addition of 50 mM 4-cyanophenylboronic acid (BA9) (middle), and the same nanotube sample after the subsequent addition of 50 mM glucose to the BA-SWNT complex.

energetically less favorable, leading to a recovery of nanotube fluorescence.

This fluorescence recovery mechanism is further supported by our observation that the emission wavelength

of (7,5) nanotubes does not recover back to the original value, even at a glucose concentration that saturates the fluorescence recovery, whereas the emission wavelength of (6,5) and (8,3) nanotubes, which have smaller

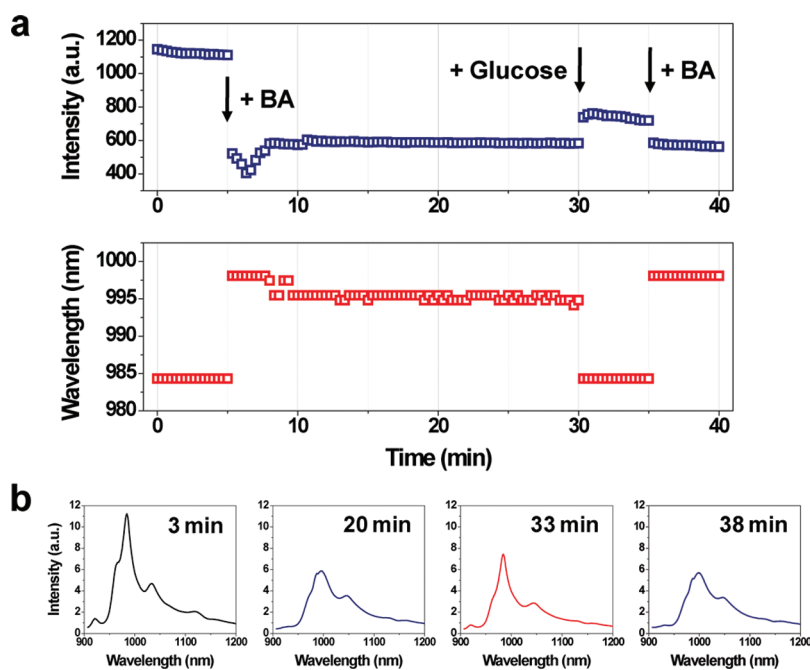


**Figure 6.** Dynamic response of nanotube fluorescence upon sequential addition of 4-chlorophenylboronic acid (BA2), glucose, and the boronic acid. (a) Peak fluorescence intensity (top) and wavelength (bottom) of (6,5) nanotubes as a function of time. (b) Corresponding fluorescence spectra at four different times (as indicated in the figures). 4-Chlorophenylboronic acid (25 mM) was introduced to the SC/SWNT solutions at 5 min, glucose (50 mM) at 30 min, and 4-chlorophenylboronic acid (25 mM) at 35 min.

diameters (larger band gaps) than (7,5) nanotubes, recovers back to the original wavelength. Since (7,5) nanotubes have a more negative conduction band potential than (6,5) and (8,3) nanotubes, the excited electron transfer from (7,5) nanotubes to the boronic acid complexed with glucose may be still energetically favorable, while the fluorescence quenching of (6,5) and (8,3) may not. The excitation profile maps for 4-cyanophenylboronic acid (BA9) clearly show this trend, along with the fluorescence recovery in the presence of glucose (Figure 5d). The observation that (7,5) nanotubes do not fully recover their emission wavelength also supports that the boronic acids complexed with glucose are likely to remain on the surface of the nanotubes.

Previous studies<sup>9</sup> reported a similar reversible quenching of SWNTs, where SWNTs interacting with a redox-active dye molecule with a ligand (biotin) show fluorescence quenching, through a similar excited-state electron transfer mechanism, and further interaction between the ligand and the target analyte (avidin) recovers the quenched fluorescence. They speculated that a strong binding affinity between the receptor (biotin) and the target analyte (avidin) can overcome the weak interaction between the ligand–dye molecule conjugate and the nanotube and thus disrupt the excited-state charge transfer pathway, leading to the nanotube fluorescence recovery.<sup>9</sup> It is a plausible mechanism, considering a large size of avidin, which is much larger than biotin and biotin–dye molecule conjugates and a strong binding affinity between avidin

and biotin.<sup>9,30</sup> In our study, however, considering a similarly small size of boronic acids and glucose and the observation that (7,5) nanotubes do not recover their emission wavelength, whereas (6,5) and (8,3) nanotubes do recover (as discussed above), the reduction potential shift of the complexed boronic acid that makes the excited electron transfer from the nanotube to the complexed boronic acid energetically less favorable is more likely responsible for the fluorescence recovery in the presence of glucose than the physical disruption of the charge transfer pathway between the nanotube and the boronic acid.

We also examined whether the binding and unbinding kinetics were fast enough to potentially enable a dynamic sensing response to glucose. Figure 6 shows the fluorescence intensity and wavelength of (6,5) nanotubes upon sequential addition of 25 mM 4-chlorophenylboronic acid (BA2) at 5 min, 50 mM glucose at 30 min, and 25 mM 4-chlorophenylboronic acid at 35 min as a function of time (Figure 6a), along with the corresponding fluorescence spectra at four different times (Figure 6b). The BA–SWNT complex shows a rapid, reversible dynamic modulation of the nanotube fluorescence upon addition of glucose and the boronic acid, indicating a fast binding and unbinding kinetics of glucose. This rapid, dynamic response of the BA–SWNT complex suggests that the reversible fluorescence quenching mechanism described in this work can potentially be used for dynamic sensing of target analytes (*e.g.*, continuous glucose monitoring).

Lastly, we attempt to understand the design rules to enable sensors of similar composition from the structure of responsive boronic acids. None of the BA–SWNT complexes of the meta-substituted phenylboronic acids (BA1, BA5, BA13, BA20, and BA24) show substantial responses to glucose: neither the BA–SWNT complexes of the boronic acids with electron-donating groups (amine (BA1), phenyl (BA13), and methoxybenzyloxy (BA20) groups) nor those with electron-withdrawing groups (nitro (BA5) and bromide (BA24) groups) are glucose-responsive. The phenyl derivative (BA13) is the only one in this subset that shows a solvatochromic shift upon initial binding; if the  $\pi$ -stacking arrangement described above is operative, biphenyl boronic acid (BA13) is the only member of the meta-substituted family that would necessarily be oriented in a different configuration. As both aromatic rings attempt to stack, this configuration may be responsible for the shift.

We found an optimal spatial configuration in the para-substituted phenylboronic acids: BA2, BA3, BA6, BA9, BA19, BA21, and BA27. The two promising candidates recognized in this work come from the electron-withdrawing subset of this family: chloro (BA2) and cyano (BA9) phenylboronic acids; these two species respond proximately to glucose. The other two electron-withdrawing, para-substituted phenylboronic acids, carboxyphenylboronic acid (BA3) and benzenediboronic acid (BA6), contain strong hydrophilic moieties in the para-position; this additional hydrophilicity would necessarily make it difficult for these species to partition into the hydrophobic surfactant adsorbed phase. The remaining family members (BA19, BA21, and BA27) are electron-donating. Therefore, one conclusion for the sensor design is that para-substituted, electron-withdrawing phenyl boronic acids can modulate SWNT fluorescence in response to glucose if they are sufficiently hydrophobic to adsorb on the nanotubes.

## METHODS

**Preparation of SWNT Suspensions and BA–SWNT Complex Solutions.** SWNTs synthesized by the CoMoCAT process (Sigma–Aldrich, 0.5 mg/mL) were sonicated in a 2% aqueous solution of sodium cholate (SC) for 20 min using a 750 W cup-horn sonicator (Vibra-Cell) at 90% amplitude. The SWNT suspension was ultracentrifuged at 30 000 rpm for 4 h, and the upper 80% of nanotube suspension was retrieved as a stable aqueous suspension of individual SWNTs functionalized by SC (SC/SWNTs). BA–SWNT complex solutions were prepared by adding boronic acids dissolved in DMSO (1 M) into the SC/SWNT solutions.

**Spectroscopy.** Near-infrared (nIR) fluorescence spectra were acquired with 785 nm excitation using a Zeiss AxioVision inverted microscope coupled to a Princeton Instruments InGaAs OMA V array detector through a PI Action SP 2500 spectrometer. Absorbance was measured using a Shimadzu UV-3101PC UV–visible–nIR scanning spectrophotometer in a cuvette with a 1 cm path length.

The naphthylboronic acids (BA4, BA7, BA10, BA11, BA12, BA14, BA22, and BA26), the anthracene-boronic acids (BA8, BA18, and BA23), and other aromaticboronic acids (BA15, BA16, BA17, BA25, BA28, BA29, and BA30) do not show strong responses to glucose, reinforcing the notion that the requisite molecular configuration appears to be para-substitution, electron-withdrawing and strong adsorption to the SWNT surface.

## CONCLUSION

We studied the reactivity of SWNTs with 30 aromatic boronic acids and the fluorescence spectral response of these 30 BA–SWNT complexes to glucose in aqueous solutions. We demonstrated that the fluorescence of the BA–SWNT complexes, quenched by the boronic acid receptor *via* an excited electron transfer mechanism, can be selectively recovered upon binding of glucose to the boronic acid receptor on the nanotubes. The BA–SWNT complex in particular modulates its fluorescence intensity with glucose concentrations in a physiologically important range of 5 to 30 mM. This “turn-on” sensing scheme, which uses the reversible fluorescence quenching and wavelength shift of the BA–SWNT complex, provides a new approach for nIR optical sensing of saccharides and glycoproteins. Since various synthetic approaches are available for the design of boronic acids with enhanced specificity and sensitivity,<sup>17,20,31,32</sup> the sensitivity and selectivity of the BA–SWNT complex to saccharides may be further improved or optimized for specific applications, and the further development of the two-component sensing approach that uses SWNTs and boronic acids as read-out units and molecular receptors, respectively, may also be extended into various biological and chemical sensing applications. One conclusion for sensor design is that para-substituted, electron-withdrawing phenyl boronic acids can modulate the SWNT in response to glucose if they are sufficiently hydrophobic to adsorb.

**High-Throughput Screening.** High-throughput screening of 30 boronic acids and the response of the 30 BA–SWNT complexes to glucose was done in a 96-well plate. The 30 BA–SWNT complex solutions were prepared by adding 10  $\mu$ L of 30 boronic acids in DMSO (1 M) to 190  $\mu$ L SC/SWNT solutions. The fluorescence spectrum of the BA–SWNT complex solutions was measured 30 min after adding boronic acids. The fluorescence spectral response of the 30 BA–SWNT complexes to glucose (50 mM) was measured 30 min after adding 10.5  $\mu$ L of glucose (1 M) to the BA–SWNT complex solutions. The equal volume of boronic acids (10  $\mu$ L) and glucose (10.5  $\mu$ L) was added to each well of SC/SWNT solutions (190  $\mu$ L). The SWNT solutions were thoroughly mixed after adding boronic acids and glucose. The solutions reached the equilibrium within several minutes after adding boronic acids and glucose. The BA–SWNT complexes and the effects of glucose were stable for at least several hours.

**Supporting Information Available:** Additional figures. This material is available free of charge *via* the Internet at <http://pubs.acs.org>.

## REFERENCES AND NOTES

- O'Connell, M. J.; Bachilo, S. M.; Huffman, C. B.; Moore, V. C.; Strano, M. S.; Haroz, E. H.; Rialon, K. L.; Boul, P. J.; Noon, W. H.; Kittrell, C.; *et al.* Band Gap Fluorescence from Individual Single-Walled Carbon Nanotubes. *Science* **2002**, *297*, 593–596.
- Bachilo, S. M.; Strano, M. S.; Kittrell, C.; Hauge, R. H.; Smalley, R. E.; Weisman, R. B. Structure-Assigned Optical Spectra of Single-Walled Carbon Nanotubes. *Science* **2002**, *298*, 2361–2366.
- Strano, M. S.; Moore, V. C.; Miller, M. K.; Allen, M. J.; Haroz, E. H.; Kittrell, C.; Hauge, R. H.; Smalley, R. E. The Role of Surfactant Adsorption during Ultrasonication in the Dispersion of Single-Walled Carbon Nanotubes. *J. Nanosci. Nanotechnol.* **2003**, *3*, 81–86.
- Barone, P. W.; Baik, S.; Heller, D. A.; Strano, M. S. Near-Infrared Optical Sensors Based on Single-Walled Carbon Nanotubes. *Nat. Mater.* **2005**, *4*, 86–92.
- Kim, J.-H.; Heller, D. A.; Jin, H.; Barone, P. W.; Song, C.; Zhang, J.; Trudel, L. J.; Wogan, G. N.; Tannenbaum, S. R.; Strano, M. S. The Rational Design of Nitric Oxide Selectivity in Single-Walled Carbon Nanotube Near-Infrared Fluorescence Sensors for Biological Detection. *Nat. Chem.* **2009**, *1*, 473–481.
- Walsh, A. G.; Vamivakas, A. N.; Yin, Y.; Cronin, S. B.; Unlü, M. S.; Goldberg, B. B.; Swan, A. K. Screening of Excitons in Single, Suspended Carbon Nanotubes. *Nano Lett.* **2007**, *7*, 1485–1488.
- Yoon, H.; Ahn, J.-H.; Barone, P. W.; Yum, K.; Sharma, R.; Boghossian, A. A.; Han, J.-H.; Strano, M. S. Periplasmic Binding Proteins as Optical Modulators of Single-Walled Carbon Nanotube Fluorescence: Amplifying a Nanoscale Actuator. *Angew. Chem., Int. Ed.* **2011**, *50*, 1828–1831.
- Heller, D. A.; Pratt, G. W.; Zhang, J.; Nair, N.; Hansborough, A. J.; Boghossian, A. A.; Reuel, N. F.; Barone, P. W.; Strano, M. S. Peptide Secondary Structure Modulates Single-Walled Carbon Nanotube Fluorescence as a Chaperone Sensor for Nitroaromatics. *Proc. Natl. Acad. Sci. U.S.A.* **2011**, *108*, 8544–8549.
- Satishkumar, B. C.; Brown, L. O.; Gao, Y.; Wang, C.-C.; Wang, H.-L.; Doorn, S. K. Reversible Fluorescence Quenching in Carbon Nanotubes for Biomolecular Sensing. *Nat. Nanotechnol.* **2007**, *2*, 560–564.
- Ahn, J.-H.; Kim, J.-H.; Reuel, N. F.; Barone, P. W.; Boghossian, A. A.; Zhang, J.; Yoon, H.; Chang, A. C.; Hilmer, A. J.; Strano, M. S. Label-Free, Single Protein Detection on a Near-Infrared Fluorescent Single-Walled Carbon Nanotube/Protein Microarray Fabricated by Cell-Free Synthesis. *Nano Lett.* **2011**, *11*, 2743–2752.
- Cognet, L.; Tsybolski, D. A.; Rocha, J.-D. R.; Doyle, C. D.; Tour, J. M.; Weisman, R. B. Stepwise Quenching of Exciton Fluorescence in Carbon Nanotubes by Single-Molecule Reactions. *Science* **2007**, *316*, 1465–1468.
- Jin, H.; Heller, D. A.; Kim, J.-H.; Strano, M. S. Stochastic Analysis of Stepwise Fluorescence Quenching Reactions on Single-Walled Carbon Nanotubes: Single Molecule Sensors. *Nano Lett.* **2008**, *8*, 4299–4304.
- Heller, D. A.; Jin, H.; Martinez, B. M.; Patel, D.; Miller, B. M.; Yeung, T.-K.; Jena, P. V.; Hobartner, C.; Ha, T.; Silverman, S. K.; *et al.* Multimodal Optical Sensing and Analyte Specificity Using Single-Walled Carbon Nanotubes. *Nat. Nanotechnol.* **2009**, *4*, 114–120.
- Heller, D. A.; Baik, S.; Eurell, T. E.; Strano, M. S. Single-Walled Carbon Nanotube Spectroscopy in Live Cells: Towards Long-Term Labels and Optical Sensors. *Adv. Mater.* **2005**, *17*, 2793–2799.
- James, T. D.; Sandanayake, K. R. A. S.; Shinkai, S. Saccharide Sensing with Molecular Receptors Based on Boronic Acid. *Angew. Chem., Int. Ed. Engl.* **1996**, *35*, 1910–1922.
- Mader, H. S.; Wolfbeis, O. S. Boronic Acid Based Probes for Microdetermination of Saccharides and Glycosylated Biomolecules. *Microchim. Acta* **2008**, *162*, 1–34.
- Shoji, E.; Freund, M. S. Potentiometric Saccharide Detection Based on the  $pK_a$  Changes of Poly(aniline boronic acid). *J. Am. Chem. Soc.* **2002**, *124*, 12486–12493.
- James, T. D.; Samankumara Sandanayake, K. R. A.; Shinkai, S. Chiral Discrimination of Monosaccharides Using a Fluorescent Molecular Sensor. *Nature* **1995**, *374*, 345–347.
- Takahashi, S.; Anzai, J.-i. Phenylboronic Acid Monolayer-Modified Electrodes Sensitive to Sugars. *Langmuir* **2005**, *21*, 5102–5107.
- Ori, A.; Shinkai, S. Electrochemical Detection of Saccharides by the Redox Cycle of a Chiral Ferrocenylboronic Acid Derivative: A Novel Method for Sugar Sensing. *J. Chem. Soc., Chem. Commun.* **1995**, 1771–1772.
- Cordes, D. B.; Gamsey, S.; Singaram, B. Fluorescent Quantum Dots with Boronic Acid Substituted Viologens To Sense Glucose in Aqueous Solution. *Angew. Chem., Int. Ed.* **2006**, *45*, 3829–3832.
- Fang, H.; Kaur, G.; Wang, B. Progress in Boronic Acid-Based Fluorescent Glucose Sensors. *J. Fluoresc.* **2004**, *14*, 481–489.
- Edwards, N. Y.; Sager, T. W.; McDevitt, J. T.; Anslyn, E. V. Boronic Acid Based Peptidic Receptors for Pattern-Based Saccharide Sensing in Neutral Aqueous Media, an Application in Real-Life Samples. *J. Am. Chem. Soc.* **2007**, *129*, 13575–13583.
- Pickup, J. C.; Hussain, F.; Evans, N. D.; Rolinski, O. J.; Birch, D. J. S. Fluorescence-Based Glucose Sensors. *Biosens. Bioelectron.* **2005**, *20*, 2555–2565.
- Kondepati, V.; Heise, H. Recent Progress in Analytical Instrumentation for Glycemic Control in Diabetic and Critically Ill Patients. *Anal. Bioanal. Chem.* **2007**, *388*, 545–563.
- Heller, D. A.; Jeng, E. S.; Yeung, T.-K.; Martinez, B. M.; Moll, A. E.; Gastala, J. B.; Strano, M. S. Optical Detection of DNA Conformational Polymorphism on Single-Walled Carbon Nanotubes. *Science* **2006**, *311*, 508–511.
- Choi, J. H.; Strano, M. S. Solvatochromism in Single-Walled Carbon Nanotubes. *Appl. Phys. Lett.* **2007**, *90*, 223114.
- O'Connell, M. J.; Eibergen, E. E.; Doorn, S. K. Chiral Selectivity in the Charge-Transfer Bleaching of Single-Walled Carbon-Nanotube Spectra. *Nat. Mater.* **2005**, *4*, 412–418.
- Zheng, M.; Diner, B. A. Solution Redox Chemistry of Carbon Nanotubes. *J. Am. Chem. Soc.* **2004**, *126*, 15490–15494.
- Chen, L.; McBranch, D. W.; Wang, H.-L.; Helgeson, R.; Wudl, F.; Whitten, D. G. Highly Sensitive Biological and Chemical Sensors Based on Reversible Fluorescence Quenching in a Conjugated Polymer. *Proc. Natl. Acad. Sci. U.S.A.* **1999**, *96*, 12287–12292.
- Wulff, G. Selective Binding to Polymers via Covalent Bonds. The Construction of Chiral Cavities as Specific Receptor Sites. *Pure Appl. Chem.* **1982**, *54*, 2093–2102.
- Kim, K. T.; Cornelissen, J. J. L. M.; Nolte, R. J. M.; van Hest, J. C. M. Polymeric Monosaccharide Receptors Responsive at Neutral pH. *J. Am. Chem. Soc.* **2009**, *131*, 13908–13909.